Structural Aspects of Long-Lived $C_7H_8^{2+}$ Dications Generated by the Electron Ionization of Toluene†

Jana Roithová,*,‡,§ Detlef Schröder,*,§ Philipp Gruene,§ Thomas Weiske,§ and Helmut Schwarz§

J. Heyrovský Institute of Physical Chemistry, Academy of Sciences of the Czech Republic, Dolejškova 3, 18223 Praha 8, Czech Republic, and Institut für Chemie der Technischen Universität Berlin, Straße des 17. Juni 135, D-10623 Berlin, Germany

Received: August 12, 2005; In Final Form: October 19, 2005

The structure of the $C_7H_8^{2+}$ dication generated upon electron ionization of toluene is investigated by experimental and theoretical means. For the long-lived $C_7H_8^{2+}$ dication, the experimental findings obtained with a novel SIFT/GIB instrument suggest complete loss of structural integrity corresponding to the toluene structure. Instead, the manifold of $C_7H_8^{2+}$ dications most likely to be formed is assigned to a mixture of the cycloheptatriene dication and ring-protonated benzylium ions.

Introduction

The structure and fragmentation patterns of neutral[1,2] and ionized[3] toluene have been extensively studied in the past. The structure of the $C_7H_8^{\bullet+}$ ions formed by the ionization of toluene depends on the internal energy deposited in the course of ionization.[4] Thus, at low internal energies (<2 eV), the ions keep the connectivity of toluene ($TOL^{\bullet+}$). For a narrow range of internal energies between 2.0 and 2.2 eV, the interconversion to the cycloheptatriene structure ($CHT^{\bullet+}$) becomes possible, whereas above 2.2 eV, the ion $C_7H_8^{\bullet+}$ already starts to lose a hydrogen atom and to enter the $C_7H_7^+$ manifold, a reaction which then rapidly predominates at higher internal energies. Consequently, the majority of the long-lived $C_7H_8^{\bullet+}$ ions formed upon ionization of toluene keep their connectivity, as has been demonstrated before by the ion−cyclotron resonance (ICR) studies of ion/molecule reactions of $C_7H_8^{\bullet+}$ ions.[5] The simplest fragmentation of the toluene monocation—loss of a hydrogen atom—either proceeds directly to the benzyl cation (Bz^+) or is associated with a series of rearrangements leading eventually to the tropylium ion (Tr^+). This process has been addressed by means of many experimental and theoretical approaches.[4−10] The barrier for the interconversion $TOL^{\bullet+} \rightarrow CHT^{\bullet+}$ lies lower in energy than the dissociation limits for the loss of a hydrogen atom from both $TOL^{\bullet+}$ and $CHT^{\bullet+}$, therefore both Bz^+ and Tr^+ are formed near the threshold. The relative ratio for the populations of Bz^+ and Tr^+ varies with the internal energy. For internal energies close to the dissociation limits, the population of Tr^+ prevails, for internal energy in excess of about 1 eV, the ratio is close to one, and with further increasing the internal energy, the formation of Bz^+ is preferred.[3,9]

The present work addresses the same structural issue for doubly ionized toluene. Caused by the usually quite energetic mode of double ionization, dications are often formed such that they contain a large amount of excess internal energy. Thus, various skeletal rearrangements can be expected, provided the associated barriers are comparably small. Moreover, the toluene dication has two low-lying electronic states, the ground-state singlet ($^1A'$) and a triplet ($^3A''$) with a spacing of the order of a tenth of an electronvolt. On the basis of theoretical data, it has been suggested that vertical ionization of neutral toluene leads to the formation of both dication states in similar amounts.[11] However, neither has the lifetime of the excited state been estimated so far nor does there exist direct experimental proof for the involvement of two electronic states in the near-threshold $C_7H_8^{2+}$ ions. As to the structure of the toluene dication,[12] early work of Meyerson[13] has suggested that hydrogen atoms from the methyl group are about four times more probable to be lost than those coming from the ring, thus suggesting a "memory" of the toluene structure. Just like with the monocation surface, however, the interplay of TOL^{2+} and CHT^{2+} structures needs to be addressed carefully and moreover even other isomers need to be considered for the doubly charged species. To tackle this challenging problem, here we present a combined experimental and theoretical study of the $C_7H_8^{2+}$ dications possibly evolving upon double ionization of neutral toluene.

Experimental and Computational Details

Sector-Field Mass Spectrometer. Initial experiments were performed with a modified VG ZAB/HF/AMD four-sector mass spectrometer of BEBE configuration (B stands for magnetic and E for electric sector), which has been described in detail previously.[14] Briefly, the dications of interest were generated by 70 eV electron ionization of the corresponding neutral precursor molecules (Chart 1), accelerated by a potential of 8 kV, and mass selected by means of B(1)/E(1). The unimolecular fragmentations of metastable ions (MI) occurring in the field-free region preceding the second magnet were monitored by scanning B(2). All spectra were accumulated with the AMD-Intectra data system; 5−15 scans were averaged to improve the signal-to-noise ratio. Final data were derived from two to four independent measurements with an experimental error smaller than ±1%.

SIFT/GIB Apparatus. The ion−molecule reactions of mass-selected $C_7H_8^{2+}$ dications (and several isotopologs) at low

† Part of the special issue "Jürgen Troe Festschrift".

* To whom correspondence should be addressed. E-mail: detlef.schroeder@tu-berlin.de.

‡ Academy of Sciences of the Czech Republic.

§ Institut für Chemie der Technischen Universität Berlin.

10.1021/jp0545288 CCC: $33.50
Published on Web 11/19/2005

CHART 1

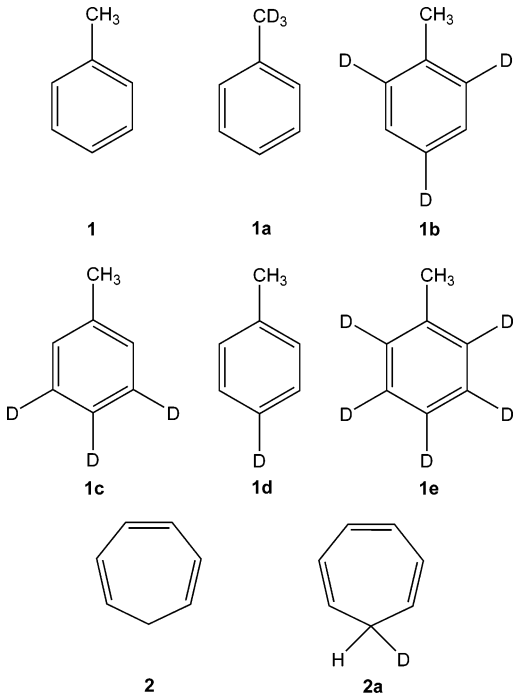

collision energies were investigated using a novel multipole device, custom-made for the Berlin laboratory by ABB Extrel. Briefly, the machine consists of a versatile ion source, followed by a quadrupole mass filter, then an ion flow tube, and then a tandem-multipole mass spectrometer (Figure 1). As such, this instrument combines the elements of a selected ion flow tube (SIFT)[15] and a guided ion beam (GIB)[16] mass spectrometer. This setup is accordingly referred to as the SIFT/GIB apparatus and is described in more detail in the following.

Ions can be produced in three different sources, via electron or chemical ionization (EI/CI), electrospray ionization (ESI), or glow-discharge ionization (GDI). The resulting ions are then mass analyzed or selected using the first quadrupole mass filter (Q1) and detected in front of the flow tube. Alternatively, either all ions emerging from the source, only a certain mass region, or just a single-mass ion can be directed toward the flow tube which they enter through a Venturi-type injector designed as recommended by Fishman and Grabowski,[17] consisting of an inner and an outer inlet in order to create a Venturi effect. Under SIFT conditions, that is in the presence of ca. 0.5 mbar helium in the flow tube, the injector is held close to zero potential relative to the ion source, to ensure a smooth entrance of the ions into the tube. In the absence of helium, however, application of a higher potential to the injector (up to ±400 V) increases ion transmission. The flow tube is 100 cm long and 7 cm in diameter with three gas inlets, 22, 44, and 66 cm behind the entrance orifice. At the end of the tube, a fraction of the ions passes through a molybdenum sampling disk, behind which an ion-extraction lens is placed for increased sampling efficiency.[18] The ions extracted from the flow tube are then directed toward the second quadrupole analyzer Q2, pass an octopole collision cell O, and then the third quadrupole Q3. An additional EI source, situated behind the SIFT extractor lens, permits us to use the back-end of the instrument also as a separate QOQ mass spectrometer.[19] The two detectors of the instrument, D1 in front of the flow tube and D2 behind the QOQ arrangement, are electron multipliers operating in either analog- or ion-counting mode. All operations including the acquisition of mass spectra are controlled by the Merlin Automation Software from ABB Extrel.

A crucial item in SIFT devices concerns appropriate differential pumping, because the pressure in the flow tube can be as high as 1 mbar, whereas the quadrupoles require a pressure of $<10^{-4}$ mbar for proper functioning. Differential pumping is maintained by seven turbomolecular pumps, backed by additional prepumps. This setup ensures pressures of 10^{-5}−10^{-7} mbar in the entire high-vacuum parts of the instrument under all operating conditions. The bulk gas from the flow tube itself is pumped at the end of the tube by an ensemble of a powerful root pump (Pfeiffer WKP 4000 A, 4050 m^3/h) sustained by a rotary vane pump (Pfeiffer UNO 250 A, 250 m^3/h), both situated in a separate room below the instrument. Pressures are measured at each pump, in addition behind the entrance and in front of the exit orifices of the flow tube and inside the octopole.

The three ion deflectors fulfill two major tasks, one is to allow the rectangular setup and the other is the improvement of function. With the first deflector, it is decided which of the three ion sources is used, while the second deflector determines whether ions are detected at D1 or allowed to enter the flow tube. The third deflector bends the ions toward the QOQ device and also serves to reduce the gas load in the back-end of the machine by improving the options for the arrangements of the vacuum pumps. The design of such deflectors has been described before.[20] Briefly, they consist of four 90° quarter sections of a round stainless steel rod, 62 mm in length and 22 mm in diameter, situated on the corners of a square. DC voltages of up to ±400 V can be applied to connected pairs of opposite electrodes. If the voltage is the same on both pairs, then ions will pass the deflector straight on, while applying a voltage of around 0 V to one pair and around −150 V to the other will result in a deflection of around 90°.

The three quadrupoles Q1−Q3 are all of same type and dimension and equipped with an entrance lens, a pre- as well as a post-filter, and an exit lens. The quadrupoles are made of stainless steel rods with 19 mm diameter and 21 cm length and are operated at 880 kHz. The nominal maximum mass is at 1000 Thompson, and the mass resolution can be increased up to $m/\Delta m = 250$, ensuring proper selection of single-mass ions, thus even of neighbored dications such as $C_7H_7^{2+}$ and $C_7H_8^{2+}$ ($m/z = 45.5$ and 46.0, respectively, see the example spectra shown below). The lenses have a 15 mm aperture and can be run with a voltage of ±400 V. All quadrupoles can work in a scan mode, radio frequency (rf)-only mode, or can be parked on a given mass in order to mass-select certain ions.

The collision experiments are performed in a rf-only octopole reaction cell which serves as an ion guide.[21] The octopole assembly has a total length of 60 cm and is split in three parts of equal dimensions of which the first and third are heavily vented, whereas the central part has a tight housing to ensure a well-defined reaction region to which neutral reagent gases are introduced. The reaction products eventually formed are effectively trapped and, as long as they are scattered in the forward direction, are mass analyzed by Q3 and then detected. The interaction energy in the ion/molecule reactions is controlled by the potential applied to the octopole housing in the MS/MS mode, and the absolute values are determined by retarding potential analysis (see the example given further below).

Theoretical Methods. The calculations were performed using the density functional method B3LYP[22−24] in conjunction with triple-ζ basis sets 6-311+G(2d,p) as implemented in the Gaussian 98 package of programs.[25] For all optimized structures,

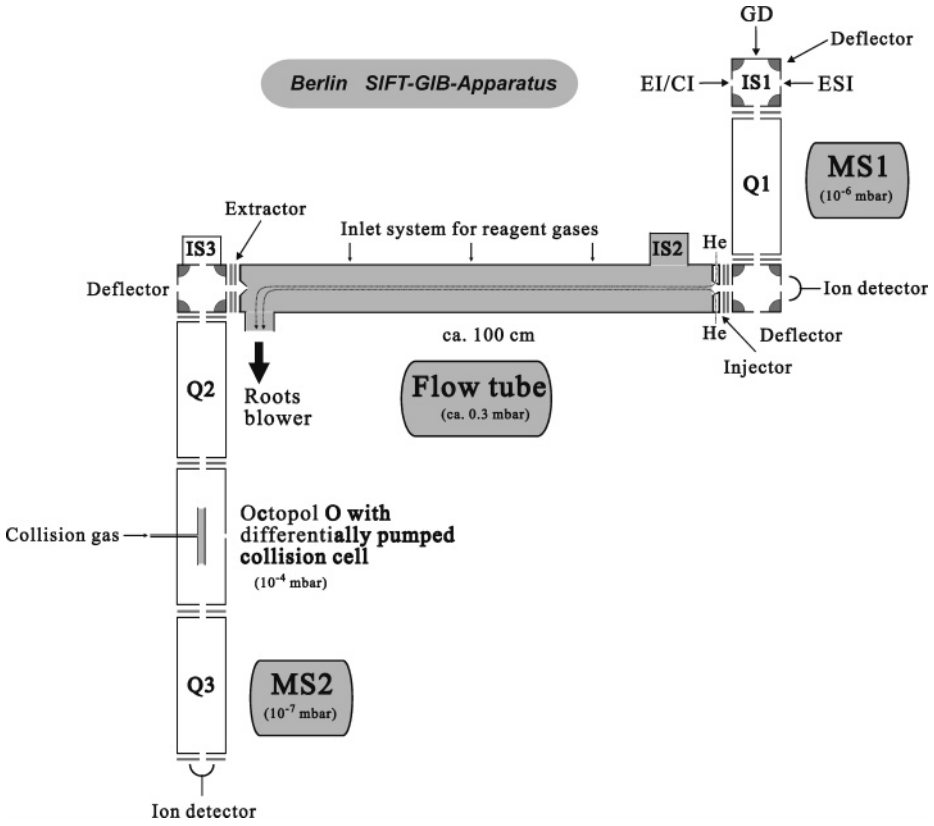

Figure 1. Schematic setup of the novel SIFT/GIB instrument installed at the TU Berlin. Briefly, ions formed in the ion source (IS1) are selected using the quadupole Q1, then directed to a flow tube which can be operated without any gas or with a helium flow at a typical pressure of 0.3 mbar, then the ions are sampled by a detection system of QOQ design (see the Experimental and Computational Details section for more information).

frequency analysis at the same level of theory was used in order to assign them as genuine minima and transition structures on the potential-energy surface (PES). In addition, the computed harmonic frequencies were used in order to calculate zero-point vibrational energy (ZPVE). The relative energies (E_{rel}) mentioned below refer to 0 K and are given in electronvolts relative to the ground state of the toluene dication ($^1\mathbf{1}^{2+}$).[26] For the $C_7H_7^+$ ions, the relative energies refer to the energy of tropylium ion ($^1\mathbf{21}^+$).[27] As far as the accuracy of the B3LYP approach is concerned, we refer to extensive studies of Pople and coworkers,[28] according to which B3LYP predicts the first ionization energies of main group compounds within ±0.1 eV. As far as second ionization energies are concerned, the absolute error of theoretical prediction is certainly somewhat larger.[29] While no comprehensive comparison of B3LYP values and experimental data has been made for dications, an accuracy of at least ±0.5 eV in absolute ionization energies appears realistic;[11,30] the relative energetics within the $C_7H_8^{2+}$ system can safely be expected to be better.

Results and Discussion

The structure as well as the possible structural diversity of the $C_7H_8^{2+}$ dications generated upon ionization of neutral toluene and also the role of electronically excited states are investigated by a combination of three methods: (i) extensive computational studies using density functional theory, (ii) analysis of the unimolecular fragmentation of $C_7H_8^{2+}$ ions in a sector mass spectrometer, and (iii) the investigation of ion/molecule reactions of long-lived $C_7H_8^{2+}$ ions using a novel multipole instrument (see Experimental and Computational Details). For conceptual reasons, let us begin with the theoretical results in order to map out the scope of the topic with which to be dealt.

Computational Results. The possible rearrangements and dissociation pathways of $C_7H_8^{2+}$ are studied by density functional calculations.[31,32] Chart 2 shows some selected structures and their energies in electronvolts relative to the toluene dication $^1\mathbf{1}^{2+}$ in the singlet state ($E_{rel} = 0.00$ eV). The cycloheptatriene dication ($^1\mathbf{2}^{2+}$) is significantly more stable with a relative energy of −0.70 eV. On the singlet surface, the nonclassical, bridged carbenium (di)cation $^1\mathbf{3}^{2+}$ is a minimum ($E_{rel} = 0.01$ eV) very close in energy to $^1\mathbf{1}^2$. Hydrogen migration from the C_1-substitutent to the ring leads to the manifold of protonated benzyl cations, of which the *meta*-protonated benzyl cation $^1\mathbf{5}^{2+}$ ($E_{rel} = -1.11$ eV) is the most stable isomer of the $C_7H_8^{2+}$ surface found in this study. *Ortho*-protonated benzyl cation $^1\mathbf{4}^{2+}$ lies only 0.17 eV higher in energy ($E_{rel} = -0.94$ eV), whereas the *para*-isomer ($^1\mathbf{4}^{2+}$) is somewhat less stable; note that the corresponding *ipso*-isomer has no minimum on the singlet surface and instead transforms to either the bridged structure $^1\mathbf{3}^{2+}$ or the *ortho*-isomer $^1\mathbf{4}^{2+}$. Some representative structures derived from five-membered rings ($\mathbf{7}^{2+}-\mathbf{10}^{2+}$) represent minima on the $C_7H_8^{2+}$ surface but are significantly higher in energy than $^1\mathbf{2}^{2+}$ and $^1\mathbf{5}^{2+}$ as well as much more remotely related to the structure of toluene and thus not considered any further. The same holds true for structures $^1\mathbf{11}^{2+}$ and $^1\mathbf{12}^{2+}$ which bear a seven-membered ring like $^1\mathbf{2}^{2+}$, but less extended π-systems, and the ring-opened representatives $^1\mathbf{13}^{2+}-{}^1\mathbf{15}^{2+}$. Accordingly, the subsequent search for the barriers associated with the mutual rearrangements and the losses of molecular hydrogen from the dications are only studied for the isomers which contain a six-membered ring ($\mathbf{1}^{2+}$, $\mathbf{3}^{2+}$, $\mathbf{4}^{2+}$, $\mathbf{5}^{2+}$, and $\mathbf{6}^{2+}$) as well as the cycloheptatriene dication $\mathbf{2}^{2+}$ (Figure 2).

The first step on the way from toluene dication $^1\mathbf{1}^{2+}$ to a more stable structure, with an either six- or seven-membered

CHART 2

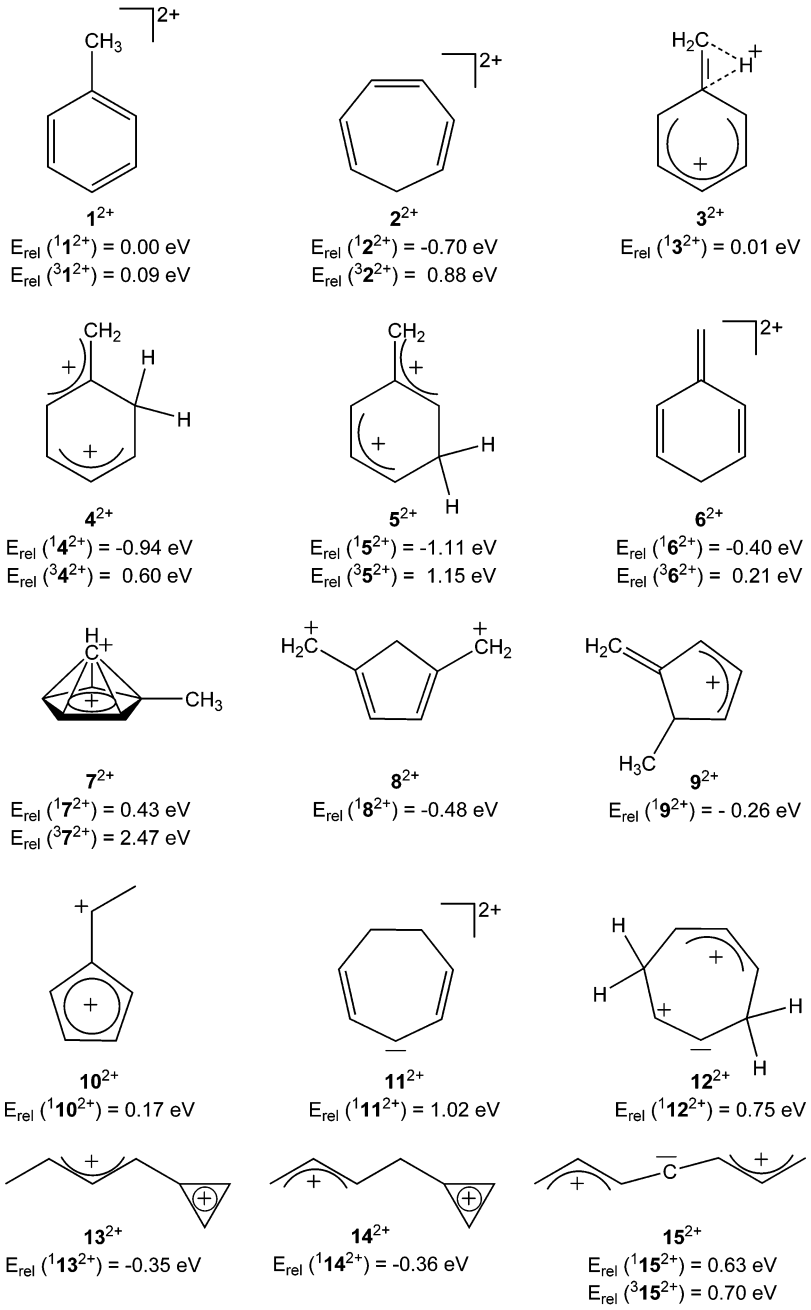

ring, consists of the migration of a hydrogen atom from the methyl group to the ring. The corresponding transition structure TS $^1\mathbf{1}^{2+}/^1\mathbf{3}^{2+}$ is associated with a very low relative energy (less than 0.01 eV) and leads to the minimum $^1\mathbf{3}^{2+}$. The geometry and also the energy (E_{rel} = 0.01 eV) of $^1\mathbf{3}^{2+}$ are very close to those of the transition structure, and it can thus be described as a π-complex between the *exo*-double bond of a benzyl cation and a proton. With the inclusion of zero-point vibrational energy, the relative energy of the minimum $^1\mathbf{3}^{2+}$ is even slightly above TS $^1\mathbf{1}^{2+}/^1\mathbf{3}^{2+}$.[33] Therefore, it can be expected that the movement of a hydrogen atom along the *exo*-C−C bond is essentially barrierless. The next step can lead either to the valley of ring-protonated benzyl cations ($^1\mathbf{4}^{2+}$−$^1\mathbf{6}^{2+}$) or to the cycloheptatriene dication $^1\mathbf{2}^{2+}$, in other words the protonated tropylium ion (TrH^{2+}). The first possibility is associated with the transition structure TS $^1\mathbf{3}^{2+}/^1\mathbf{4}^{2+}$; it has an activation energy of E_{rel}(TS $^1\mathbf{3}^{2+}/^1\mathbf{4}^{2+}$) = 0.21 eV. As mentioned above, the *ortho*- and *meta*-protonated benzyl cations represent the most stable structures which were found for the $C_7H_8^{2+}$ dication. The rearrangement of the toluene dication via minimum $^1\mathbf{3}^{2+}$ to the cycloheptatriene dication is associated with a barrier situated at E_{rel}(TS $^1\mathbf{2}^{2+}/^1\mathbf{3}^{2+}$) = 0.51 eV.

The most abundant fragmentation of the metastable $C_7H_8^{2+}$ dication observed experimentally corresponds to a loss of molecular hydrogen.[34] The direct 1,1-dehydrogenation of the toluene dication to the benzylidene dication $^1\mathbf{16}^{2+}$ requires 2.23 eV (Chart 3). In comparison, direct 1,1-dehydrogenation of the cycloheptatriene dication $^1\mathbf{2}^{2+}$ is much less energy demanding, and the corresponding dissociation limit lies at E_{rel}($^1\mathbf{17}^{2+}$ + H_2) = 1.22 eV. The dehydrogenations of the protonated benzyl cations $\mathbf{4}^{2+}$−$\mathbf{6}^{2+}$ require energies between these two extremes, with the lowest one corresponding to E_{rel}($^1\mathbf{20}^{2+}$ + H_2) = 1.67 eV. Given the computational prediction that the highest barrier separating isomers $\mathbf{1}^{2+}$−$\mathbf{6}^{2+}$ on the singlet surface amounts to E_{rel} = 0.51 eV associated with TS $^1\mathbf{2}^{2+}/^1\mathbf{3}^{2+}$, we can therefore conclude that the metastable $C_7H_8^{2+}$ ions nascent from ionization

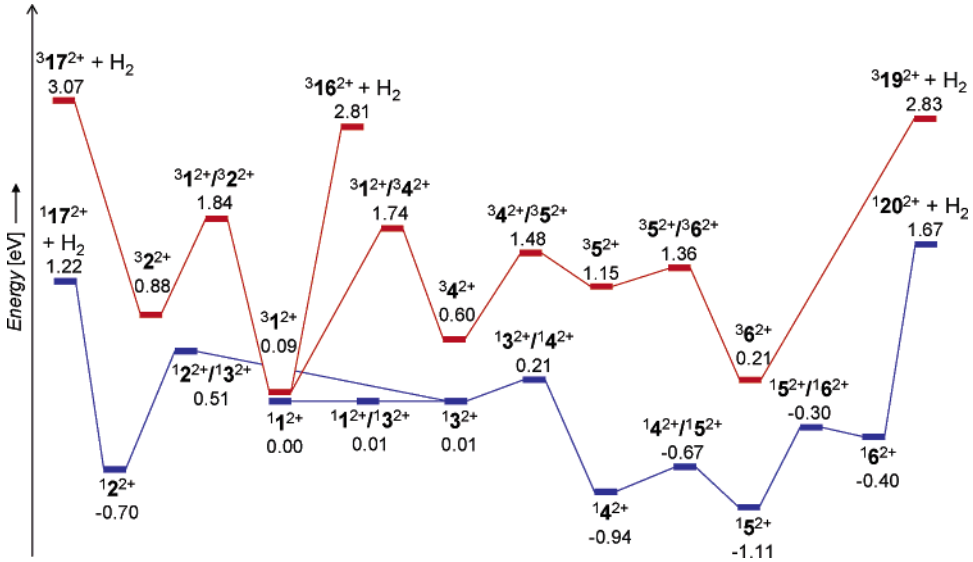

Figure 2. Relevant potential-energy surface (in electronvolts) of $C_7H_8^{2+}$ ions generated by double ionization of neutral toluene, **1**. The $C_7H_8^{2+}$ surface is shown for singlet (blue) and triplet (red) states including the toluene structure ($\mathbf{1}^{2+}$), the isomeric cycloheptatriene dication ($\mathbf{2}^{2+}$), and the protonated benzylium ions ($\mathbf{4}^{2+}$−$\mathbf{6}^{2+}$), as well as energetically low-lying dehydrogenation pathways.

CHART 3

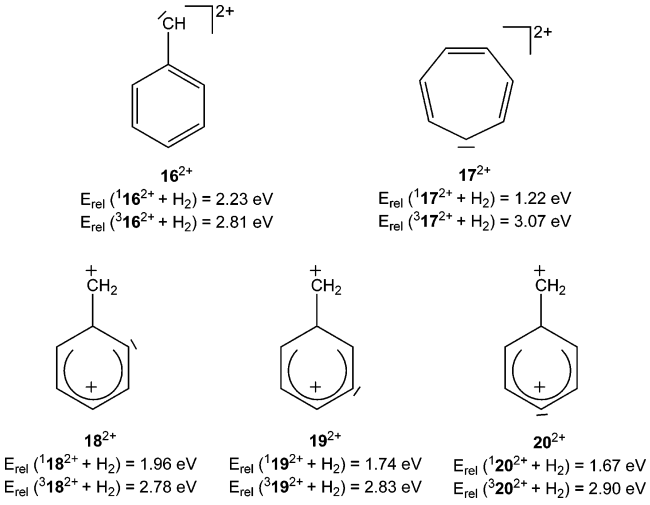

of toluene follow the least energy-demanding route to $^1\mathbf{17}^{2+}$ + H_2. Moreover, with the barriers separating the various isomers situated well below the lowest-lying dissociation channel, rapid interconversion of the isomers and equilibration of any eventual isotopic labeling prior to dissociation is implied.

As to the triplet state of $C_7H_8^{2+}$, the most stable structure corresponds to the isomer $^3\mathbf{1}^{2+}$ with E_{rel} = 0.09 eV. All other triplet structures lie considerably higher in energy, as can be seen in Chart 1. The lifetime of $^3\mathbf{1}^{2+}$ can be influenced by possible fragmentations or by spin crossover which would lead to the singlet surface. The direct dehydrogenation of the toluene dication in the triplet state leads to a rather high dissociation limit of E_{rel} = 2.81 eV. The other possible fragmentations proceeding via rearrangements of $^3\mathbf{1}^{2+}$ to other isomers of toluene dication lead to dissociations limits, which lie even higher in energy (Chart 3). Moreover, the rearrangements of the toluene dication in the triplet state themselves lead to considerably less stable isomers, and they are also associated with high energy barriers (Figure 2). The migration of a hydrogen atom from the methyl group to the ring, which leads to the valley of the ring-protonated benzyl cation in the triplet state, is prevented by a barrier of 1.74 eV. Similarly, the rearrangement to the protonated tropylium ion in the triplet state is hindered by a barrier of 1.84 eV. Accordingly, it is expected that the spin crossover to the singlet surface is more efficient in a possible depletion of the triplet state than the various dissociation reactions conceivable.

From theoretical studies of the phenyl cation[35] and its *para*-substituted derivatives,[36] it has been concluded that the spin isomerization takes place in the region of crossing of the ground and the excited potential-energy surfaces.[37] Moreover, it has been suggested that the minimum energy crossing points (MECPs), similar to the transition states, follow Hammond's postulate.[38] Thus, when the excited state is much higher in energy than the ground state, the MECP lies close to the excited state, both in energy and in geometry. Consequently, even though the probability of spin interconversion might be low, the excited state frequently passes the MECP which finally leads to a high overall spin isomerization rate. On the other hand, for the ground state and the excited state lying close in energy, whereas their geometries differ significantly, as it is the case of $^1\mathbf{1}^{2+}$ and $^3\mathbf{1}^{2+}$,[11] the MECP may give rise to a barrier. Usually, a spin isomerization is encountered as well, but the lifetime of the excited state may be substantially longer than that in the first case.[36] Furthermore, the symmetries of the wave functions corresponding to the $^1\mathbf{1}^{2+}$ and $^3\mathbf{1}^{2+}$ dications are different (^{1}A′ and ^{3}A″, respectively), and consequently, the zeroth-order spin−orbit coupling element between the triplet and singlet states of the toluene dication vanishes, and spin crossover is hence even less efficient. Accordingly, it can be expected that the lifetime of $^3\mathbf{1}^{2+}$ may suffice to allow its observation in experiments using the microsecond time scale.[39]

For the sake of completeness, also the monocationic $C_7H_7^+$ species possibly evolving from $C_7H_8^{2+}$ upon dissociative charge transfer are considered and their relative energies are given in Chart 4. The B3LYP method applied here predicts the cycloheptatrienylium ion $\mathbf{21}^+$ as the most stable isomer with the benzylium ion $\mathbf{22}^+$ somewhat less stable; the tolylium ions $\mathbf{23}^+$−$\mathbf{25}^+$ as well as the protonated benzylidenes $\mathbf{26}^+$−$\mathbf{28}^+$ are at least 2 eV higher in energy.

In resuming the theoretical predictions, it is expected that the dehydrogenation of the toluene dication in the singlet state preferentially proceeds via the sequence $^1\mathbf{1}^{2+} \rightarrow {}^1\mathbf{3}^{2+} \rightarrow {}^1\mathbf{2}^{2+}$

CHART 4

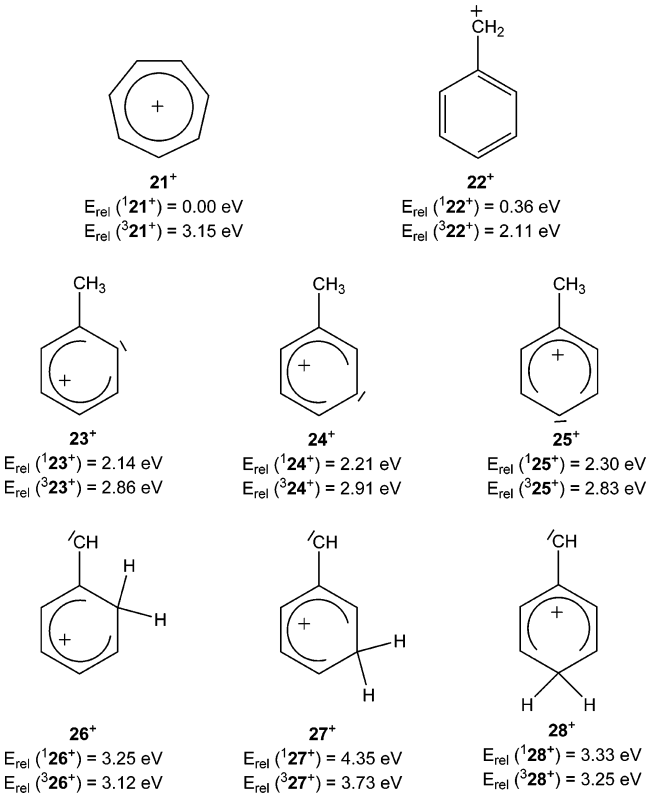

$\rightarrow {}^1\mathbf{17}^{2+} + H_2$. This mechanism further implies complete hydrogen scrambling prior to the dehydrogenation via the isomers ${}^1\mathbf{2}^{2+}-{}^1\mathbf{6}^{2+}$. If the dehydrogenation takes place from the manifold of protonated benzyl cations, then a higher abundance of ring-hydrogen atoms in the eliminated hydrogen molecule than those coming originally from the methyl group should be observed in the experiment. The presence of the triplet states of the toluene cation in the beam of mass-selected $C_7H_8^{2+}$ should lead to a relative decrease of H_2 elimination, because it is expected that dehydrogenation occurs preferentially at the singlet potential-energy surface.

Experimental Results. The $C_7H_8^{2+}$ ions investigated in the experiments described here are generated by electron ionization of neutral toluene and cycloheptatriene, respectively. It has been shown that the photoionization of toluene above the ionization thresholds of both the singlet and triplet states of $C_7H_8^{2+}$ yields about a 1:1 mixture of ${}^1\mathbf{1}^{2+}$ and ${}^3\mathbf{1}^{2+}$;[11] due to the lack of more precise information, as a first approximation, we expect the formation of a similar mixture in the case of electron ionization.[40,41] In contrast, electron ionization of cycloheptatriene most likely yields preferentially $C_7H_8^{2+}$ in the singlet state, because the triplet state lies 1.58 eV higher in energy.

$$C_7H_8^{2+} \rightarrow C_7H_6^{2+} + H_2 \qquad (1)$$

The metastable ion spectra obtained in the sector-field mass spectrometer show exclusive loss of molecular hydrogen for all $C_7H_8^{2+}$ ions investigated here (eq 1). However, the abundance of H_2 loss relative to the intensity of the parent-dication $C_7H_8^{2+}$ generated from toluene is $3.6 \pm 0.1\%$, whereas the same process for the dication generated from cycloheptatriene is substantially more abundant, that is, $6.6 \pm 0.1\%$. A straightforward rationale for this experimental finding involves the population of the triplet state upon the EI of toluene, which relatively decreases the abundance of dehydrogenation, provided that spin isomerization is slow in the microsecond regime of the sector-field experiments. Nevertheless, also quasi-irreversible rearrangements of ${}^1\mathbf{1}^{2+}$ to the ring-protonated benzyl cations (${}^1\mathbf{4}^{2+}-{}^1\mathbf{6}^{2+}$) may account for the experimental findings as their dissociation limits are higher in energy (Chart 3).

TABLE 1: Isotopic Distribution Observed in the Unimolecular Dehydrogenation of Mass-selected $C_7H_5D_3^{2+}$ Dications Formed upon EI of the D_3-labeled, Neutral Toluenes 1a, 1b, and 1c[a]

	$-H_2$	$-HD$	$-D_2$
$\mathbf{1a}^{2+}$	45.6	47.8	6.5
$\mathbf{1b}^{2+}$	45.6	47.8	6.6
$\mathbf{1c}^{2+}$	46.0	47.5	6.5
model[b]	45.8	47.6	6.6

[a] The intensities are given relative in percent, and the error is less than 0.5%. [b] Kinetic modeling including a statistical weighting of the propensities for H_2, HD, and D_2 losses as well as a kinetic isotope effect of 1.44 per D atom involved.

Isotopic labeling has often been used in order to experimentally probe ion structures. To this end, the metastable ion spectra of several labeled $C_7H_{8-n}D_n^{2+}$ ions (Chart 1) are considered. Experimentally, it turns out that the ratios of $H_2/HD/D_2$ eliminations are identical within the error margins for all D_3-labeled dications studied here (Table 1). This finding implies a complete scrambling of the H(D) atoms prior to dehydrogenation. The experimental data can satisfactorily be reproduced by a simple kinetic modeling[42] which acknowledges the statistical propensities of H_2, HD, and D_2 losses and includes a kinetic isotope effect of KIE = 1.44 per deuterium atom directly involved in the reaction. Accordingly, the dehydrogenation must proceed via rearrangement to a common intermediate, most likely the cycloheptatriene dication as suggested by the calculations discussed above. Nevertheless, these results only demonstrate that the metastable fraction of the $C_7H_8^{2+}$ dications has undergone complete equilibration, but this may not hold true for the majority of long-lived, non-decomposing ions emerging from the ion source. The entire population of ions can be sampled in collision experiments at kiloelectronvolt energies. However, the differences observed in the fragment ions in the charge-exchange spectra of $C_7H_5D_3^{2+}$ ions with oxygen as the collision gas are small, yet in the expected direction. Thus, for $C_7H_5D_3^{2+}$ generated from the CD_3 compound **1a**, the amount of $C_7H_5D_2^+$ is slightly larger (43% relative to $C_7H_4D_3^+$) than that for the same ion generated from ring-labeled **1b** ($C_7H_5D_2^+$ represents 40% relative to $C_7H_4D_3^+$), as expected for a preferential direct cleavage of a benzylic C−H(D) bond upon fragmentation of a dication still having the toluene structure, that is, ${}^3\mathbf{1}^{2+}$.

Accordingly, the role of protonated tropylium ions and ring-protonated benzyl cations is further elucidated by ion/molecule reactions. Hydrogen-containing dications are usually strong proton donors.[19,43,44] As a monitoring reaction, the proton transfer between the $C_7H_8^{2+}$ dication and the CO molecule has been chosen here. Equations 2−5 show the energy balances of proton transfer between various isomers of $C_7H_8^{2+}$ and CO with protonation taking place at the carbon atom of carbon monoxide ($PA^C(CO) = 6.16$ eV).[45] All of these reactions are exothermic by at least 3 eV. If the less stable isomers of the $C_7H_7^+$ product (Chart 4) are taken into consideration, the exothermicity of proton transfer decreases considerably and the processes may even become endothermic. Therefore, it can be concluded that proton transfer from $C_7H_8^{2+}$ dications to CO leads mainly, if

not exclusively, to either a benzyl cation or tropylium ion.

$$TOL^{2+}\ (^1\mathbf{1}^{2+}) + CO \rightarrow Bz^+ + HCO^+ \quad \Delta E = -4.74\ eV \tag{2}$$

$$TOL^{2+}\ (^3\mathbf{1}^{2+}) + CO \rightarrow Bz^+ + HCO^+ \quad \Delta E = -3.08\ eV \tag{3}$$

$$BzH^{2+}\ (^1\mathbf{5}^{2+}) + CO \rightarrow Bz^+ + HCO^+ \quad \Delta E = -3.64\ eV \tag{4}$$

$$CHT^{2+}\ (^1\mathbf{2}^{2+}) + CO \rightarrow Tr^+ + HCO^+ \quad \Delta E = -4.40\ eV \tag{5}$$

Chemical reactions of dications are usually in competition with facile electron transfer from the dication to a neutral reactant. The ionization energy of CO amounts to 14.01 eV, whereas the second ionization energy of toluene is 14.8 eV;[11] therefore, electron transfer is only 0.8 eV exothermic. The calculated ionization energies of other $C_7H_8^{\bullet+}$ isomers are even lower than 14 eV, which means that the electron transfer with CO would be endothermic. According to the reaction-window concept,[46] electron transfer from a neutral target to a dication is only kinetically favored when the exothermicity is larger than 2 eV.[47] As this is not the case for the system investigated here, proton transfer is expected to predominate in the reaction of mass-selected $C_7H_8^{2+}$ with CO. In perfect agreement with this line of reasoning, for the $C_7H_8^{2+}$ dications generated from both toluene and cycloheptatriene, only proton transfer to carbon monoxide to yield HCO^+ but no electron transfer is observed experimentally (see below).

The ratio between H^+ and D^+ transfer can provide information on a structural memory effect of the cation under investigation.[48] In contrast to the MI experiments described above, such an approach samples the entire manifold of the mass-selected ion beam and not just the metastable fraction. Thus, if the $C_7H_8^{2+}$ dication is at least partially present in the structure of toluene, a significant contribution of hydrogen atoms from the methyl group to proton transfer should be encountered. On the other hand, the ring-protonated benzyl cations $^1\mathbf{4}^{2+}-^1\mathbf{6}^{2+}$ should favor the transfer of hydrogen atoms originally bonded to the ring carbons, because proton transfer from the methylene group is less favorable (Chart 4). Rearrangement of $C_7H_8^{2+}$ to the seven-membered ring of cycloheptatriene is, in turn, expected to be associated with the complete scrambling of all hydrogen atoms, and thus no positional preference should be observed in the proton-transfer reactions.

To address this question, a novel SIFT/GIB device was used (see Experimental and Computational Details section). In the present experiments, the $C_7H_8^{2+}$ dications generated by electron ionization of neutral toluene and cycloheptatriene, respectively, were mass selected by means of Q1, directed through the flow tube, re-selected with Q2, and then reacted with neutral CO in the octopole region (Figure 1). The reaction products eventually formed are then mass analyzed by means of Q3 and detected. Figure 3 shows a representative mass spectrum for the $C_7H_5D_3^{2+}$ dication generated from neutral **1a**. In these experiments, the mass resolution in parent-ion selection was sufficient to completely separate $C_7H_5D_3^{2+}$ ($m/z = 47.5$) from $C_7H_4D_3^{2+}$ ($m/z = 47.0$) generated by dissociative ionization. Further note that the mass resolution of the quadrupole Q3, which is scanned in these particular experiments, allows a clear-cut distinction of H^+ and D^+ transfers (see insets in Figure 3). The product ions in Figure 3 can be assigned to three categories: (i) products of proton transfer between the dication and CO, thus $HCO^+ + C_7H_4D_3^+$ and $DCO^+ + C_7H_5D_2^+$, respectively, (ii) collision-induced dissociation (CID) of the dication via losses of H_2, HD, and D_2, respectively, and (iii) subsequent fragmentations of the singly charged product ions with patterns characteristic of $C_mH_n^+$ fragments. Note again that direct electron transfer from CO to $C_7H_8^{2+}$ is not observed at all, as demonstrated by the absence of a signal at $m/z = 95$, corresponding to $C_7H_5D_3^+$ (see right-hand inset in Figure 3).

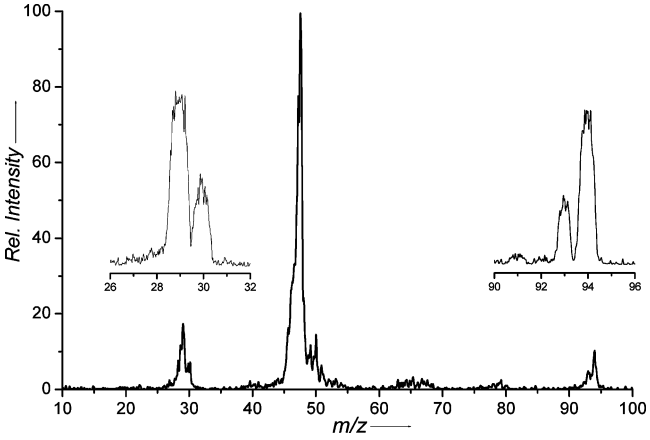

Figure 3. Representative mass spectrum of an ion/molecule reaction investigated in the SIFT/GIB instrument. Here, the $C_7H_5D_3^{2+}$ dications generated by double ionization of neutral **1a** are mass selected using Q1, transferred through the flow tube, selected again by means of Q2, reacted with carbon monoxide in the octopole collision cell, and the product ions are mass-analyzed using Q3. The left- and right-hand insets show the mass regions corresponding to H^+ and D^+ transfer at improved resolution in separate scans. Note the nicely complementary ratios of HCO^+/DCO^+ ($m/z = 29$ and 30) and $C_7H_5D_2^+/C_7H_4D_3^+$ ($m/z = 93$ and 94).

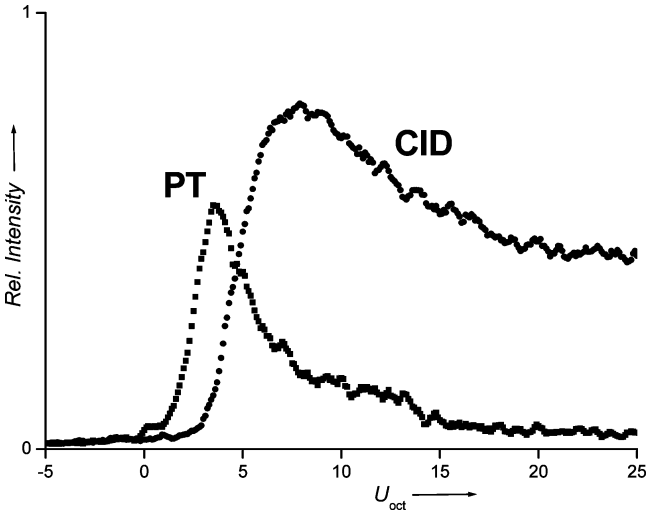

Figure 4. Relative intensity of proton transfer (PT) and collision-induced dissociation (CID) in the ion/molecule reaction of mass-selected $C_7H_8^{2+}$ dications, generated by double ionization of neutral toluene, with carbon monoxide as a function of the voltage applied to the octopole collision cell (U_{oct} in volts). As expected for an exothermic ion/molecule reaction, PT shows a sharp maximum at low energies, whereas CID has a delayed threshold and remains at larger energies.

Another important feature in a GIB device is the ability to investigate ion/molecule reactions at variable collision energies. As a representative example, Figure 4 shows the relative amounts of proton transfer (PT) and CID for $C_7H_8^{2+}$ interacting with neutral CO as a function of collision energy. As expected for an exothermic ion/molecule reaction, PT shows a maximum at low collision energy and then rapidly decreases in abundance

TABLE 2: Relative Abundances of H^+ and D^+ transfer in the Ion/Molecule Reactions of Mass-selected $C_7H_{8-n}D_n^{2+}$ with Carbon Monoxide in the Octopole Reaction Chamber[a]

	experiment[b]		model[c]	
	$[CO,H]^+$	$[CO,D]^+$	$[CO,H]^+$	$[CO,D]^+$
$\mathbf{1a}^{2+}$	70 ± 5	30 ± 5	70	30
$\mathbf{1b}^{2+}$	70 ± 1	30 ± 1	70	30
$\mathbf{1d}^{2+}$	87 ± 1	13 ± 1	91	9
$\mathbf{1e}^{2+}$	50 ± 1	50 ± 1	46	54
$\mathbf{2a}^{2+}$	89 ± 2	11 ± 2	91	9

[a] The intensities are given relative in percent. [b] Errors derived from averaging of several independent experiments. [c] Kinetic modeling including a statistical weighting of the propensities for H^+ vs D^+ transfer and a kinetic isotope effect of 1.4 for D^+ transfer.

at higher energies. The opposite holds true for the CID products, which start with a somewhat delayed onset but then remain approximately constant in the energy regime studied here, forming a kind of plateau.

With respect to the structural questions outlined above, we are particularly interested in the PT to carbon monoxide and thus the ratio of HCO^+ and DCO^+ formed in the reactions of (labeled) $C_7H_{8-n}D_n^+$ dications with CO. The experimental results obtained for various isotopomers of the toluene dication are listed in Table 2. The identical findings for D_3 isotopomers $\mathbf{1a}^{2+}$ and $\mathbf{1b}^{2+}$ suggest that complete scrambling is indeed the case. Similarly, D_1 isotopomers of the dications generated from toluene and cycloheptatriene yield the same results within experimental error. In agreement, a purely statistical model with inclusion of a kinetic isotope effect of KIE = 1.4 associated with intermolecular PT gives values that are close to those obtained in the measurements (Table 2). At first sight, these results appear to contradict the significant differences with regard to the unimolecular dehydrogenation of the $C_7H_8^{2+}$ dications generated from either toluene or cycloheptatriene, respectively (see above). Note, however, that different time scales are sampled in both kinds of experiments. Thus, in the sector experiments, ion selection and fragmentation occurs in the lower microsecond regime, whereas the time the ions travel in the SIFT/GIB device from the ion source to the octopole region is in the order of milliseconds (even tenths of a second in the presence of helium). Therefore, we conclude that during the flight time elapsing in the SIFT prior to reaching the reaction in the octopole, the $C_7H_8^{2+}$ dications undergo complete equilibration of all H(D) atoms and thus form the same mixtures of isomers disregarding the structure of the neutral precursor used.

How do these experimental results compare with the theoretical findings? A rationalization again involves a significant population of the triplet state $^3\mathbf{1}^{2+}$ upon double ionization of toluene. With spin isomerization occurring in the microsecond regime, the results in the sector field can be attributed to a mixture of singlet and triplet $C_7H_8^{2+}$, whereas in the course of the much longer time-of-flight elapsing in the SIFT/GIB device, conversion to the singlet spin ground state is complete with the formation of the energetically low-lying structures $^1\mathbf{2}^{2+}$, $^1\mathbf{4}^{2+}$, and $^1\mathbf{5}^{2+}$ as the most likely major components.

Last, but not least, this system can be used to probe whether organic dications, having a sizable recombination energy, can at all be probed in a SIFT apparatus or if nonavoidable impurities in the gas-supply systems prevent an effective collisional cooling of such dications. In fact, previous SIFT studies of dications involved species which have relatively low recombination energies, such as Ca^{2+} or dications of polycyclic aromatic hydrocarbons and fullerenes.[30,49,50] With a species such as $C_7H_8^{2+}$, particularly the notorious impurities O_2 and H_2O pose problems, because electron and proton transfer are likely to occur. Specifically, in the case of oxygen, the ionization energy of $IE(O_2) = 12.1$ eV renders electron transfer according to eq 6 exothermic by more than 2 eV, thus perfectly fulfilling the requirements of the reaction-window concept. Charge transfer with oxygen (and thus residual air) is therefore expected to be rather efficient. Likewise, proton transfer with water (eq 7) is expected to be efficient because $PA(H_2O) = 7.2$ eV even exceeds that of CO, for which proton transfer already is predominant (see above).

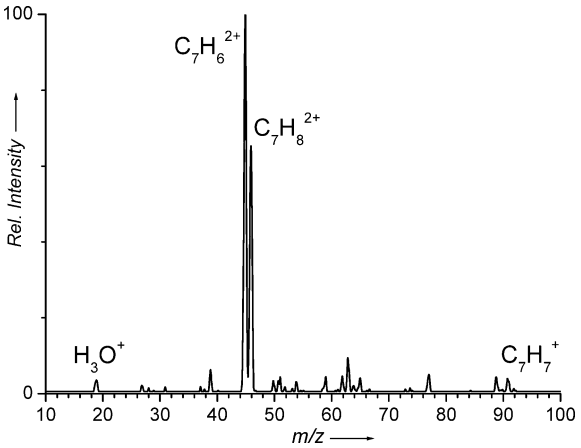

Figure 5. Representative mass spectrum of mass-selected $C_7H_8^{2+}$ dications passing through the flow tube of the SIFT/GIB instrument operated at a pressure of 0.3 mbar helium. Note that the major signals correspond to the dicationic species (the $C_7H_8^{2+}$ precursor and the CID product $C_7H_6^{2+}$), whereas monocationic products which could arise from impurities in the helium are of low abundance.

$$C_7H_8^{2+} + O_2 \rightarrow C_7H_8^{+} + O_2^{+\bullet} \quad (6)$$

$$C_7H_8^{2+} + H_2O \rightarrow C_7H_7^{+} + H_3O^{+} \quad (7)$$

Moreover, $C_7H_8^{2+}$ poses a specific problem due to the relatively facile dehydrogenation of the dication according to eq 1. Hence, with the effects of possible impurities in the vacuum system aside, the injection of the mass-selected ion beam into the flow tube region might be associated with a considerable amount of fragmentation.

The spectrum shown in Figure 5 demonstrates that, despite all these various obstacles, the SIFT/GIB device is indeed suitable for the examination of an organic dication such as $C_7H_8^{2+}$. Here, $C_7H_8^{2+}$ was mass selected by means of Q1, injected into the flow tube operating at 0.3 mbar helium pressure, and mass analyzed and detected in the QOQ system. Quite to our surprise, it turns out that impurities in the vacuum system play only a minor role (see the products H_3O^+ and $C_7H_7^+$ in Figure 5). Instead, the major reason for losses in $C_7H_8^{2+}$ intensity is due to the CID in the injector region according to eq 1. Considering the above finding that the long-lived $C_7H_8^{2+}$ ions have lost their memory, we have not further pursued reactivity studies of these ions emerging from the flow tube in operation but want to point out the principal function of the new apparatus.

Conclusion

In previous work, it had been shown that near-threshold double ionization of neutral toluene leads the corresponding dication as a mixture of singlet and triplet states.[11] Here, a combination of theoretical and experimental methods is used

to investigate the possible rearrangements of the dicationic species and to probe the dication structure by mass spectrometric means. The experimental and theoretical results suggest that the short-lived $C_7H_8^{2+}$ ions sampled in sector-field experiments exist as a mixture of singlet and triplet states. The structure of long-lived $C_7H_8^{2+}$ ions generated from toluene is investigated by a novel multipole instrument in which the reactions of deuterium-labeled $C_7H_{8-n}D_n^{2+}$ ions with carbon monoxide are studied. At low kinetic energies, only proton and deuteron transfer are observed and the ratios of the HCO^+ and DCO^+ products are independent of the original position of the label in the neutral toluene serving as a precursor. Hence, the ion/molecule reactions suggest that all ions collapse to a single structure or a common mixture of isomers. This conclusion is consistent with the computational results which predict isomeric structures (either cycloheptratriene dication or protonated benzylium ions) are more stable than the toluene dication itself and the connecting barriers are relatively low in energy. Furthermore, the results suggest that the lifetime of the triplet states is long enough to allow the probe of their presence in experiments sampling the microsecond regime, whereas complete conversion to the more stable singlet states is achieved in the flight times of several milliseconds elapsing in the multipole experiments. In this context, a few other aspects related to the performance of the novel SIFT/GIB instrument are addressed.

Acknowledgment. Generous support by the Deutsche Forschungsgemeinschaft, the Grant Agency of the Academy of Sciences of the Czech Republic (No. KJB4040302), and the Fonds der Chemischen Industrie is gratefully acknowledged. We are particularly indebted to the late Mr. Richard Schaeffer from ABB Extrel, without whose help the complete performance of the SIFT/GIB instrument could not have been achieved. This work is dedicated to Professor Jürgen Troe on the occasion of his 65th birthday.

References and Notes

(1) Hippler, H.; Reihs, C.; Troe, J. *Z. Phys. Chem.* **1990**, *167*, 1.

(2) Brouwer, L. D.; Mueller-Markgraf, W.; Troe, J. *J. Phys. Chem.* **1988**, *92*, 4905.

(3) Lifshitz, C. *Acc. Chem. Res.* **1994**, *27*, 138.

(4) Lifshitz, C.; Gotkis, Y.; Ioffe, A.; Laskin, J.; Shaik, S. *Int. J. Mass Spectrom. Ion Processes* **1993**, *125*, R7.

(5) Hoffman, M. K.; Bursey, M. M. *Tetrahedron Lett.* **1971**, *12*, 2539.

(6) Howe, I.; McLafferty, F. W. *J. Am. Chem. Soc.* **1971**, *93*, 99.

(7) Dewar, M. J. S.; Landman, D. *J. Am. Chem. Soc.* **1977**, *99*, 2446.

(8) Bombach, R.; Dannacher, J.; Stadelmann, J.-P. *J. Am. Chem. Soc.* **1983**, *105*, 4205.

(9) Fridgen, T. D.; Troe, J.; Viggiano, A. A.; Midey, A. J.; Williams, S.; McMahon, T. B *J. Phys. Chem. A* **2004**, *108*, 5600.

(10) Fati, D.;. Lorquet, A. J.; Locht, R.; Lorquet, J. C.; Leyh, B. *J. Phys. Chem. A* **2004**, *108*, 9777.

(11) Roithová, J.; Schröder, D.; Loos, J.; Schwarz, H.; Jankowiak, H.-Ch.; Berger, R.; Thissen, R.; Dutuit, O. *J. Chem. Phys.* **2005**, *122*, 094306.

(12) Fati, D.; Leyh, B. *Eur. J. Mass Spectrom.* **2003**, *9*, 223.

(13) Meyerson, S. *J. Am. Chem. Soc.* **1963**, *85*, 3340.

(14) Srinivas, R.; Sülzle, D.; Weiske, T.; Schwarz, H. *Int. J. Mass Spectrom. Ion Processes* **1991**, *107*, 368.

(15) Adams, N. G.; Smith, D. *Int. J. Mass Spectrom. Ion Phys.* **1976**, *21*, 349.

(16) Armentrout, P. B. *J. Am. Soc. Mass Spectrom.* **2002**, *13*, 419.

(17) Fishman, V. N.; Grabowski, J. J. *Int. J. Mass Spectrom.* **1998**, *177*, 175.

(18) Van Doren, J. M. Ph.D. Thesis, University of Colorado, Boulder, CO, **1987**.

(19) Roithová, J.; Herman, Z.; Schröder, D.; Schwarz, H. *Chem.−Eur. J.*, in press.

(20) Mahaffy, P. R.; Lai, K. *J. Vac. Sci. Technol., A* **1990**, *8*, 3244.

(21) Gerlich, D. *Adv. Chem. Phys.* **1992**, *82*, 1.

(22) Vosko, S. H.; Wilk, L.; Nusair, M. *Can. J. Phys.* **1980**, *58*, 1200.

(23) Lee, C.; Yang, W.; Parr, R. G. *Phys. Rev. B* **1988**, *37*, 785.

(24) Miehlich, B.; Savin, A.; Stoll, H.; Preuss, H. *Chem. Phys. Lett.* **1989**, *157*, 200.

(25) Frisch, M. J.; Trucks, G. W.; Schlegel, H. B.; Scuseria, G. E.; Robb, M. A.; Cheeseman, J. R.; Zakrzewski, V. G.; J. A. Montgomery, J.; Stratmann, R. E.; Burant, J. C.; Dapprich, S.; Millam, J. M.; Daniels, A. D.; Kudin, K. N.; Strain, M. C.; Farkas, O.; Tomasi, J.; Barone, V.; Cossi, M.; Cammi, R.; Mennucci, B.; Pomelli, C.; Adamo, C.; Clifford, S.; Ochterski, J.; Petersson, G. A.; Ayala, P. Y.; Cui, Q.; Morokuma, K.; Malick, D. K.; Rabuck, A. D.; Raghavachari, K.; Foresman, J. B.; Cioslowski, J.; Ortiz, J. V.; Baboul, A. G.; Stefanov, B. B.; Liu, G.; Liashenko, A.; Piskorz, P.; Komaromi, I.; Gomperts, R.; Martin, R. L.; Fox, D. J.; Keith, T.; Al-Laham, M. A.; Peng, C. Y.; Nanayakkara, A.; Gonzalez, C.; Challacombe, M.; Gill, P. M. W.; Johnson, B. G.; Chen, W.; Wong, M. W.; Andres, J. L.; Head-Gordon, M.; Replogle, E. S.; Pople, J. A. *Gaussian 98*, revision A.11; Gaussian, Inc.: Pittsburgh, PA, 1998.

(26) $E_{tot}(^1\mathbf{1}^{2+}) = -270.789739$ hartree, ZPVE = 0.121441 hartree

(27) $E_{tot}(^1\mathbf{21}^{+}) = -270.7479976$ hartree, ZPVE = 0.118524 hartree

(28) Curtiss, L. A.; Raghavachari, K.; Redfern, P. C.; Pople, J. A. *J. Chem. Phys.* **2000**, *112*, 7374 and references therein.

(29) Petrie, S. *J. Chem. Phys.* **1997**, *107*, 3042.

(30) Schröder, D.; Loos, J.; Schwarz, L.; Thissen, R.; Preda, D. V.; Scott, L. T.; Frach, M. V.; Böhme, D. K. *Helv. Chim. Acta* **2001**, *84*, 1625.

(31) The comparative studies of theoretical and experimental heats of formations of various molecules show that the absolute accuracy of the B3LYP calculations is usually higher than ±0.2 eV.[32] However, for the potential-energy surface as described here, the errors are expected to be of a systematic manner. The relative errors in energy between various minima on the single PES will be smaller than 0.1 eV.

(32) Bauschlicher, C. W., Jr.; Ricca, A.; Partridge, H.; Langhoff, S. R. In *Recent Advances in Density Functional Methods, Part II*; Chong, D. P., Ed.; World Scientific Publishing Company: Singapore, 1997; p 165.

(33) The MP2 method even leads to the single minimum corresponding to isomer $^1\mathbf{3}^{2+}$, and isomer $^1\mathbf{1}^{2+}$ could not be located.

(34) Feil, S.; Echt, O.; Głch, K.; Hasan, V. G.; Matt-Leubner, S.; Tepnual, T.; Grill, V.; Bacher, A.; Scheier, P.; Märk, T. D. *Chem. Phys. Lett.* **2005**, *411*, 366.

(35) Harvey, J. N.; Aschi, M.; Schwarz, H.; Koch, W. *Theor. Chem. Acc.* **1998**, *99*, 95.

(36) Aschi, M.; Harvey, J. N. *J. Chem. Soc., Perkin Trans.* **1999**, *2*, 1059.

(37) For a review on the role of spin in gas-phase ion chemistry, see: Schwarz, H. *Int. J. Mass Spectrom.* **2004**, *237*, 75.

(38) Carreon-Macedo, J.-L.; Harvey, J. N.; Poli, R. *Eur. J. Inorg. Chem.* **2005**, 2999, and references therein.

(39) Roithová, J.; Schröder, D.; Berger, R.; Schwarz, H. *J. Phys. Chem. A*, in press.

(40) Samson, J. A. R. *Phys. Rev. Lett.* **1990**, *65*, 2861.

(41) See also: Harper, S.; Calandra, P.; Price, S. D. *Phys. Chem. Chem. Phys.* **2001**, *3*, 741.

(42) For similar approaches using kinetic modeling, see: (a) Loos, J.; Schröder, D.; Zummack, W.; Schwarz, H.; Thissen, R.; Dutuit, O. *Int. J. Mass Spectrom.* **2002**, *214*, 105. (b) Trage, C.; Schröder, D.; Schwarz, H. *Organometallics* **2003**, *22*, 693 (addendum **2003**, *22*, 1348). (c) Schlangen, M.; Schröder, D.; Schwarz, H. *Helv. Chim. Acta* **2005**, *88*, 1405.

(43) Roithová, J.; Žabka, J.; Thissen, R.; Herman, Z. *Phys. Chem. Chem. Phys.* **2003**, *5*, 2988.

(44) Roithová, J.; Hrušák, J.; Herman, Z. *Int. J. Mass Spectrom.* **2003**, *228*, 497.

(45) Hunter, E. P.; Lias, S. G. *J. Phys. Chem. Ref. Data* **1998**, *27*, 413.

(46) (a) Landau, L. *Phys. Z. Sowjetunion* **1932**, *2*, 46. (b) Zener, C. *Proc. R. Soc. London A* **1932**, *137*, 696. (c) Olson, R. E.; Smith, F. T.; Bauer, E. *Appl. Opt.* **1971**, *10*, 1848. (d) Salop, A.; Olson, R. E. *Phys. Chem.* **1976**, *13*, 1312.

(47) Petrie, S.; Javahery, G.; Wincel, H.; Bohme, D. K. *J. Am. Chem. Soc.* **1993**, *115*, 6290.

(48) Schröder, D.; Loos, J.; Schwarz, H.; Thissen, R.; Dutuit, O. *J. Phys. Chem. A* **2004**, *108*, 9931 and references therein.

(49) Spears, K. G.; Fehsenfeld, F. C. *J. Chem. Phys.* **1972**, *56*, 5698.

(50) Bohme, D. K. *Can. J. Chem.* **1999**, *77*, 1453 and references therein.